Accepted Manuscript

Nitrobenzofurazan derivatives of *N′*-hydroxyoximidines as potent inhibitors of indoleamine-2,3-dioxygenase 1

Saurav Paul, Ashalata Roy, Suman Jyoti Deka, Subhankar Panda, Vishal Trivedi, Debasis Manna

PII: S0223-5234(16)30459-7

DOI: 10.1016/j.ejmech.2016.05.061

Reference: EJMECH 8653

To appear in: *European Journal of Medicinal Chemistry*

Received Date: 1 March 2016

Revised Date: 25 May 2016

Accepted Date: 26 May 2016

Please cite this article as: S. Paul, A. Roy, S.J. Deka, S. Panda, V. Trivedi, D. Manna, Nitrobenzofurazan derivatives of *N′*-hydroxyoximidines as potent inhibitors of indoleamine-2,3-dioxygenase 1, *European Journal of Medicinal Chemistry* (2016), doi: 10.1016/j.ejmech.2016.05.061.

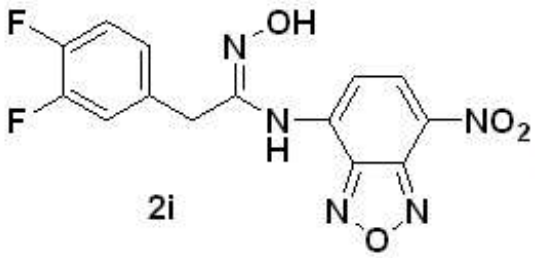

2i

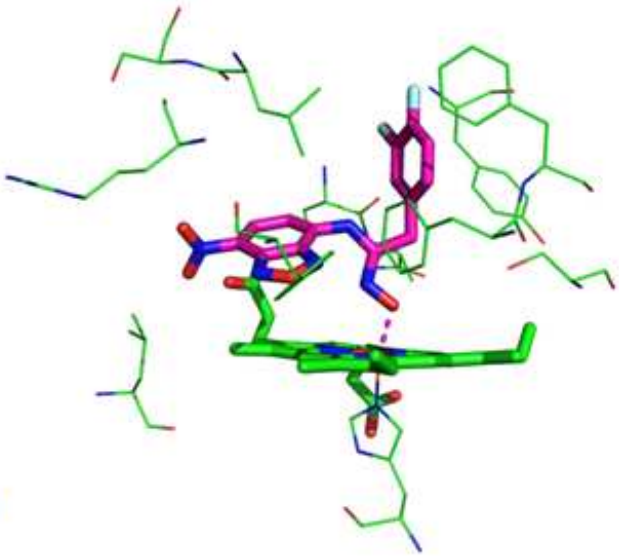

IDO1, IC_{50} = 59 nM

TDO, IC_{50} = 94 µM

Ligand efficiency = 0.405

MDA-MB-231, IC_{50} = 50 nM

Nitrobenzofurazan Derivatives of *N′*-Hydroxyoximidines as potent Inhibitors of Indoleamine-2,3-Dioxygenase 1

Saurav Paul,[‡,a] Ashalata Roy,[‡, a] Suman Jyoti Deka,[b] Subhankar Panda,[a] Vishal Trivedi *,[b] and Debasis Manna*,[a]

[a]*Department of Chemistry, Indian Institute of Technology Guwahati, Assam 781039, India*

[b]*Department of Bioscience and Bioengineering, Indian Institute of Technology Guwahati, Assam 781039, India*

Corresponding Author

Department of Chemistry, Indian Institute of Technology Guwahati, Assam-781039, India. E-mail: dmanna@iitg.ernet.in; Fax: +91 03 61258 2350; Tel: +91 03 61258 2325.

ABBREVIATIONS USED

IDO1, indoleamine 2,3-dioxygenase 1; TDO, tryptophan 2,3-dioxygenase; *L*-Trp, *L*-tryptophan; HTS, High throughput screening; UV-Vis, ultraviolet-visible; HPLC, high-performance liquid chromatography.

Abstract

Tryptophan metabolism through the kynurenine pathway is considered as a crucial mechanism in immune tolerance. Indoleamine 2,3-dioxygenase 1 (IDO1) plays a key role in tryptophan catabolism in the immune system and it is also considered as an important therapeutic target for the treatment of cancer and other diseases that are linked with kynurenine pathway. In this study, a series of nitrobenzofurazan derivatives of *N′*-hydroxybenzimidamides (**1**) and *N′*-hydroxy-2-phenylacetimidamides (**2**) were synthesized and their inhibitory activities against human IDO1 enzyme were tested using in-vitro and cellular enzyme activity assay. The optimization leads to the identification of potent compounds, **1d**, **2i** and **2k** (IC_{50} = 39-80 nM), which are either competitive or uncompetitive inhibitors of IDO1 enzyme. These compounds also showed IDO1 inhibition potencies in the nanomolar range (IC_{50} = 50-71 nM) in MDA-MB-231 cells with no/negligible amount of cytotoxicity. The stronger selectivity of the potent compounds for IDO1 enzyme over tryptophan 2,3-dioxygenase (TDO) enzyme (312 to 1593-fold) also makes them very attractive for further immunotherapeutic applications.

KEYWORDS

N′-Hydroxyoximidines, Mechanism-based drug design, IDO1 inhibition, high selectivity, low cytotoxicity.

1. Introduction

Cancer immunotherapy by targeting indoleamine 2,3-dioxygenase 1 (IDO1) and tryptophan 2,3-dioxygenase (TDO) enzymes is considered as an exciting approach for drug development [1, 2]. Both IDO1 and TDO enzymes catalyze the initial and rate limiting step in the catabolism of L-tryptophan (*L*-Trp) to *N*-formylkynurenine by oxidative cleavage of the pyrrole ring through kynurenine pathway [3, 4]. Uncontrolled metabolism of *L*-Trp abets tumor cells to escape from the immune responses [1, 4]. Reduction in local concentrations of *L*-Trp and uninhibited formation of kynurenine and other metabolites, including neurotransmitters serotonin and melatonin, excitotoxin quinolinic acid, N-methyl-D-aspartate receptor antagonist kynurenic acid, and the production of nicotinamide adenine dinucleotide (NAD) assists IDO1 enzyme to suppress the local immune response by hindering the proliferation of T-lymphocyte in the G1-phase of the cell cycle [1, 2, 5, 6]. Cytokines like interferon-γ are primarily responsible for the over-expression of IDO1 enzyme in the macrophages, epithelial and dendritic cells [7]. TDO enzyme is mainly expressed in the liver and catabolizes more than 90% of the *L*-Trp. This catabolism of *L*-Trp in the liver by the TDO enzyme systematically regulates *L*-Trp balance in response to dietary intake. The over-expression of IDO1 enzyme is interconnected with poor prognosis in different cancers, including, ovarian and pancreatic [1, 3, 8]. However, recently it is reported that endothelial IDO1 expression in kidney tumors is associated with a better prognosis [9, 10]. Cellular IDO1 activities are also related with neurodegenerative disorder HIV-1 encephalitis and age related cataract [1, 11-14].

Recent studies demonstrated that inhibition of IDO1 activity with small molecules successfully restrain the abnormal growth of tumors and also showed complemented effect with chemotherapeutic and radiotherapeutic treatment of malignant tumors [6, 15]. TDO enzyme is highly selective and preferably binds to *L*-Trp. Whereas, the active site of IDO1 enzyme is amenable to small molecules. Hence, IDO1 has emerged as an attractive target in cancer immunotherapy. Presently, two IDO1 inhibitors, INCB024360 and NLG919 are under clinical trials for the treatment of cancer and other diseases [16]. Even though 1-D-MT is under clinical trial as kynurenine pathway inhibitor but its mechanism of action is doubtful. Although, it is reported that D-1MT inhibit the kynurenine production at high concentrations but 1-D-MT does not effectively restore IDO-induced arrest of T-cell proliferation [1, 16-19]. Therefore, developments of small molecule-based IDO1 inhibitors are essential to satisfactorily address this cancer immunotherapeutic opportunity.

Incyte Corporation identified *N*-hydroxyamidines as reversible and potent inhibitors of IDO1 enzyme. One of the most potent compounds 4-amino-*N*-(3-chloro-4-fluorophenyl)-*N′*-hydroxy-1,2,5-oxadiazole-3-carboxymidimade (**5l**) showed IC_{50} values of 67 and 19 nM for in-vitro and cellular enzyme activity assay, respectively [20]. This potent compound lowered blood plasma level of kynurenine and restricted tumor growth in a mouse model. *N*-hydroxyamidine moiety containing compound INCB024360 is currently under clinical trial for the treatment of several types of cancer and other diseases [1, 16]. Compound CBR703 with *N*-hydroxyamidine moiety notably alter the activity of RNA polymerase from bacteria [21]. *N*-hydroxyamidines can be also used as pro-drugs of amidines, which is an important tool in drug discovery [5]. Therefore,

hydroxyamidine-based compounds show several biological activities and found to be a useful drug scaffold. So far there are no other reports on the modifications of hydroxyamidine scaffold for the improvement of IC_{50} values (for IDO1 enzyme inhibitory activity) of the compounds like 4-amino-*N*-(3-chloro-4-fluorophenyl)-*N′*-hydroxy-1,2,5-oxadiazole-3-carboxymidimade (**5l**) [20].

Here, we investigated IDO1 enzyme inhibitory activity by a series of *N′*-hydroxyamidine moiety containing nitrobenzofurazan derivatives. Interestingly, the resulting compounds proved to be potent inhibitors of IDO1 enzyme with inhibitory potency in the nanomolar range under *in vitro* conditions. Selected compounds also showed strong IDO1 enzyme inhibitory activity in MDA-MB-231 cells and almost no/negligible amount of toxicity at the cellular level. Additional counter screening against TDO enzyme showed their selectivity for IDO1 enzyme.

2. Results and Discussion

2.1. *Chemistry*

High throughput screening (HTS) by Incyte Corporation led to the discovery of hydroxyamidine-based potent, competitive inhibitors of IDO1 enzyme [1, 20]. Hydroxyamidine containing compound INCB024360 in combination with pembrolizumab is now in phase-I/II clinical trials for the treatment of several types of cancers [1]. The other hydroxyamidine-based potent compound, 4-amino-*N*-(3-chloro-4-fluorophenyl)-*N′*-hydroxy-1,2,5-oxadiazole-3-carboxymidimade (**5l**) showed enzymatic and cellular IC_{50} values of 67 and 19 nM (in Hela cell), respectively and inhibit melanoma growth in a mouse model [20]. A thorough structure–activity-relationship

(SAR) studies revealed that the oxygen atom of these hydroxyamidines interact with the heme-iron and play a decisive role in inhibiting IDO1 activity. Model structure also proposed that the substitute phenyl ring of compound INCB024360 or **5l** placed itself in the hydrophobic "pocket-A", whereas the furazan ring interacts with the 7-propionate of the heme-group of IDO1 enzyme [1, 20]. Detailed mechanistic studies suggested that addition of ferrous heme iron coordinated molecular oxygen across the C2-C3 double bond is the prerequisite for the IDO1 promoted oxidative cleavage of *L*-Trp in extrahepatic tissues. These studies also proposed the formation of alkylperoxy transition/intermediate state or dioxetane intermediate state during the transformation of *L*-Trp to *N*-formylkynurenine by IDO1 enzyme [1, 16].

In our attempt to synthesize compounds containing hydroxyamidine scaffold with better inhibitory potencies and to mimic the alkylperoxy transition/intermediate state, we developed a series of nitrobenzofurazan derivatives of substituted *N'*-hydroxybenzimidamides (**1**) and *N'*-hydroxy-2-phenylacetimidamides (**2**), where one oxygen atom of the peroxo-moiety is substituted with a nitrogen atom (Fig. 1). We hypothesized that substituted hydroxybenzimidamides and hydroxy-2-phenylacetimidamides would be placed inside the hydrophobic "pocket A" and interact with heme iron and can act as a mimic of the alkylperoxy transition/intermediate state for the transformation of *L*-Trp to *N*-formylkynurenine by IDO1 enzyme. Whereas, the benzofurazan moiety may interact with the 7-propionate of the heme group. The compounds **1** and **2** were synthesized in two steps under mild conditions. First, condensation of hydroxylamine with corresponding benzonitrile and phenylacetonitrile under basic condition produced substituted *N'*-hydroxybenzimidamide and *N'*-hydroxy-2-

phenylacetimidamides with good yields [22, 23]. Further treatment of these hydroxyamidines with 4-chloro-7-nitrobenzofurazan (NBD-Cl) in the presence of $NaHCO_3$ under ethanolic solution produced the target compounds **1** and **2** with moderate to good yields (Scheme 1) [24].

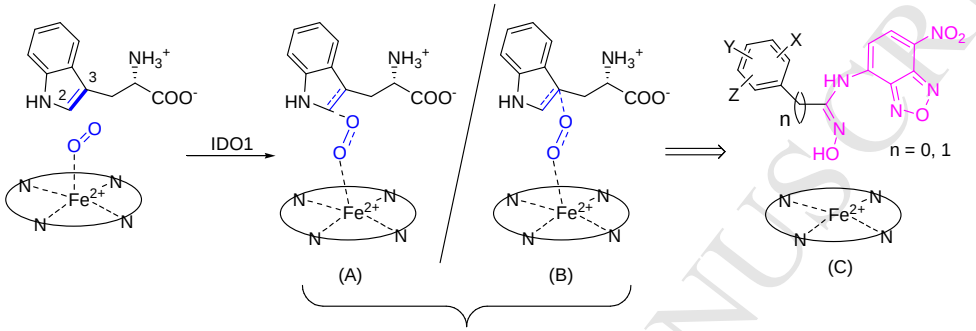

Fig. 1. Proposed alkylperoxy transition/intermediate state of IDO1 (A and B) and its mimic (C).

2.2. *Inhibitory activities of hydroxyamidines against purified IDO1 enzyme*

The potencies of the synthesized nitrobenzofurazan derivatives in inhibiting the human IDO1 enzyme activity were initially evaluated by measuring the changes in absorbance values of the product produced from kynurenine and 4-dimethylaminobenzaldehyde (at 480 nm) in acidic medium [25-27]. Uv-Vis spectra of the pure compounds (50 nM to 1μM) showed no or little interference with the activity assay. The measured K_m and k_{cat} values of the purified hIDO1 enzyme with the L-Trp as substrate were 47.8 ± 2.5 μM and 3.7 ± 0.1 s^{-1}, respectively. In an effort to further improve the efficacy of the nitrobenzofurazan derivatives of *N′*-hydroxyamidines, we explored two general modifications of the *N′*-hydroxyamidine structure: (1) modification of the carbon linker

between the aryl ring and *N′*-hydroxyamidine moiety; (2) substitution of the aryl ring (Fig.1).

Scheme 1: Synthesis of nitrobenzofurazan derivatives of *N′*-hydroxybenzimidamides and *N′*-hydroxy-2-phenylacetimidamides.

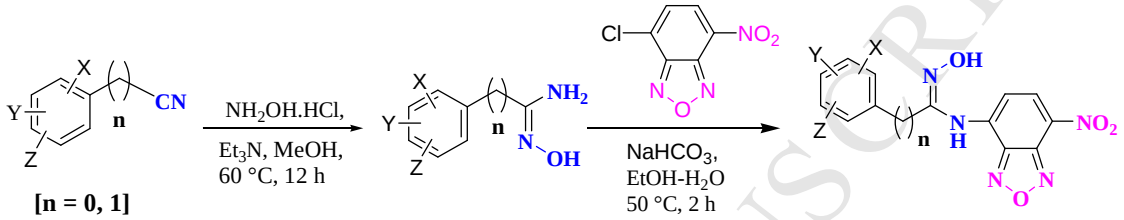

2.2.1. *Modification of the carbon linker between the aryl ring and N′-hydroxyamidine moiety*

We explored the role linker length and flexibility between the aryl ring and *N′*-hydroxyamidine moiety on the potencies of the compounds (Table 1). The IC_{50} values of compounds **1a** and **2a** against purified IDO1 enzyme clearly suggest that the incorporation of an additional methylene group between the aryl ring and *N′*-hydroxyamidine moiety resulted in a slender decrease in its inhibitory efficacy.

2.2.2. *Substitution of the aryl ring*

The effect of substitutions on the aryl ring was investigated for potential interactions with the hydrophobic residues positioned within the “pocket-A”, by incorporating methyl or halogen substitutions. Several research groups had successfully exploited these hydrophobic interactions in the optimization of the IDO1 inhibition efficacies [1, 26, 28-30]. Table 2 and 3 shows the IC_{50} values of nitrobenzofurazan derivatives of the

substituted *N'*-hydroxybenzimidamides (**1a-n**) and *N'*-hydroxy-2-phenylacetimidamides (**2a-k**), respectively. The IC_{50} value of the reported potent compound **5l** under the experimental conditions was 91 nM (Table 3), which is in accordance with the reported values [20]. The *N'*-hydroxybenzimidamide compounds, **1b-n** displayed strong hIDO1

Table 1: Inhibitory activity of the nitrobenzofurazan derivatives of *N'*-hydroxybenzimidamide and *N'*-hydroxy-2-phenylacetimidamide against purified human IDO1 enzyme.

Compound	IDO1 inhibition IC_{50} (nM)[a]	Ligand efficiency (LE) = 1.4 × pIC_{50}/HAC[b]
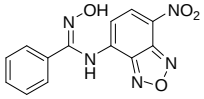 **1a**	268 ± 23	0.418
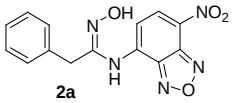 **2a**	307 ± 22	0.396

[a]IC_{50} values are the mean of five independent assays.
[b]HAC = heavy atom count.

inhibitory activities with IC_{50} values ranging from 63 to 204 nM (Table 2). The SAR studies demonstrated that halogen substituted phenyl derivative **1b, 1d**, **1f**, **1j** and **1n** have stronger IDO1 enzyme inhibition capabilities than the other synthesized *N'*-hydroxybenzimidamides. Among these tested *N'*- hydroxybenzimidamides derivatives, ortho-fluoro **1b** showed stronger hIDO1 inhibitory activity (IC_{50} = 63 nM) than original benzimidamide lead **1a**. A substantial preference for the fluoro-substitution at the ortho- (**1b**) meta- (**1f**) and para- (**1j**) positions of the phenyl ring was also observed from IDO1 enzyme inhibition studies. Various other substitutions showed moderate inhibition potencies but with IC_{50} values still in the nanomolar range. Further optimizations

revealed that di-halogen (3-Br, 4-F) substituted compound, **1n** showed stronger IDO1 inhibition potency [20]. However, other disubstituted compound, **1m** failed to show stronger inhibition efficiency. Nitrobenzofurazan derivatives of *N'*-hydroxy-2-phenylacetimidamides, **2b-k** also exhibited strong hIDO1 inhibitory activities with IC_{50} values ranging from 39 to 307 nM (Table 3). The SAR studies demonstrated that halogen-substituted benzyl derivatives **2b**, **2f**, **2i** and **2k** were more potent than the original benzyl lead **2a**. Among these tested *N'*-hydroxy-2-phenylacetimidamide derivatives, 3,4-dichloro substituted compound, **2k** showed (IC_{50} = 39 nM) stronger hIDO1 inhibitory activity than the lead compound **2a** (IC_{50} = 307 nM). 3,4-Difluoro substituted compound **2i** showed (IC_{50} = 59 nM) stronger hIDO1 inhibition potency than unsubstituted parent compound, **2a**. Preference for fluoro-substitution at meta-, ortho- and para- positions were also demonstrated by the modest improvement in hIDO1 enzyme inhibitory activity. Interestingly 3,4-dichloro-substitution (**2k**) considerably enhances the hIDO inhibitory potency than its respective mono substituted derivatives (**2d**, **2f**). Similarly, synergistic effect of 3,4-difluoro substitution was also observed for compound (**2j**).

All of these IDO1 inhibition studies were performed by spectrophotometric technique. For further confirmation of their efficacies, IDO1 activity assay was also performed by HPLC analysis. The amount of kynurenine generated due to the catabolism of *L*-Trp, was directly quantified by HPLC analysis [28]. A standard curve generated from pure kynurenine under similar experimental conditions was used to calculate the

Table 2: Inhibitory activity of the nitrobenzofurazan derivatives of *N′*-hydroxybenzimidamides against purified human IDO1 enzyme.

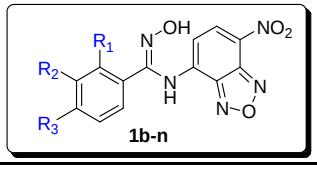

1b-n

Compound	IDO1 inhibition IC_{50} (nM)[a]	Ligand efficiency (LE) = 1.4 × pIC_{50}/HAC[b]
1b R_1 = F; R_2 = R_3 = H	63 ± 3	0.438
1c R_1 = Cl; R_2 = R_3 = H	135 ± 17	0.418
1d R_1 = Br; R_2 = R_3 = H	80 ± 6	0.431
1e R_1 = H; R_2 = CH_3; R_3 = H	163 ± 8	0.413
1f R_1 = H; R_2 = F; R_3 = H	75 ± 5	0.433
1g R_1 = H; R_2 = Cl; R_3 = H	184 ± 6	0.410
1h R_1 = H; R_2 = Br; R_3 = H	105 ± 3	0.425
1i R_1 = R_2 = H; R_3 = CH_3	204 ± 11	0.407
1j R_1 = R_2 = H; R_3 = F	100 ± 9	0.426
1k R_1 = R_2 = H; R_3 = Cl	113 ± 7	0.423
1l R_1 = R_2 = H; R_3 = Br	117 ± 1	0.422
1m R_1 = H; R_2 = Cl; R_3 = F	158 ± 26	0.397
1n R_1 = H; R_2 = Br; R_3 = F	92 ± 1	0.411

[a]IC_{50} values are the mean of five independent assays.
[b]HAC = heavy atom count.

inhibitory activity of the compounds. The calculated concentrations of the compounds required to inhibit the kynurenine production from the *L*-Trp were in the nanomolar range (Table S1) and in accordance with the measured IC_{50} values calculated using the pDMAB-method. The IC_{50} values of compounds **1b**, **1d**, **1j**, **2i** and **2k** (as measured by

HPLC method) are within 49-64 nM which is lower than the reported potent compound **5l**, under the similar experimental conditions [20].

Therefore, most of the compounds displayed stronger hIDO1 inhibitory activities. The common characteristic of these compounds is that, all of them possess nitrobenzofurazan and *N′*-hydroxyamidine moieties, which emerge to be critical for their stronger hIDO1 inhibitory activity. Separate inhibition activity studies with 4-chloro-7-nitrobenzofurazan and 2-(3,4-difluorophenyl)-*N′*-hydroxyacetimidamide, a precursor for compound **2i** showed very weak or no inhibition of IDO1 enzyme activity under the similar experimental conditions (data not shown here). This implies the importance of both nitrobenzofurazan and *N′*-hydroxybenzimidamides or *N′*-hydroxy-2-phenylacetimidamide moiety for stronger inhibition of hIDO1 activity. The compounds from **1a-n** and **2a-k** families are separated by one methylene group. Although the structures of the compounds from both the series are highly related, but their IC_{50} values indicate a substantial differences among their inhibition activities against purified IDO1 enzyme. However, the IC_{50} values of the compounds suggest that the strong interaction of *N′*-hydroxy or nitrobenzofurazan moiety of the compounds with the IDO1 enzyme could suppress the effect of substitution on the phenyl ring of *N′*-hydroxybenzimidamides or N'-hydroxy-2-phenylacetimidamides. ESI-MS spectral analyses of the selected potent compounds in water, 100 mM phosphate buffer at pH 6.5 and enzymatic assay solution revealed that these compounds are also stable under the experimental conditions (Supporting Information, Fig. S1-S5).

Table 3: Inhibitory activity of the nitrobenzofurazan derivatives of *N'*-hydroxy-2-phenylacetimidamides against purified human IDO1 enzyme

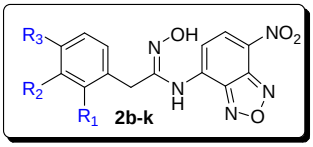

Compound	IDO1 inhibition IC_{50} (nM)[a]	Ligand efficiency (LE) = 1.4 × pIC_{50}/HAC[b]
2b R_1 = F; R_2 = R_3 = H	102 ± 5	0.408
2c R_1 = H; R_2 = F; R_3 = H	131 ± 4	0.401
2d R_1 = H; R_2 = Cl; R_3 = H	199 ± 11	0.391
2e R_1 = R_2 = H; R_3 = OCH_3	128 ± 3	0.386
2f R_1 = R_2 = H; R_3 = Cl	127 ± 1	0.402
2g R_1 = R_2 = H; R_3 = Br	112 ± 7	0.405
2h R_1 = R_2 = H; R_3 = F	98 ± 10	0.409
2i R_1 = H; R_2 = R_3 = F	59 ± 5	0.405
2j R_2 = H; R_1 = R_3 = F	160 ± 12	0.380
2k R_1 = H; R_2 = R_3 = Cl	39 ± 1	0.415
5l[c] 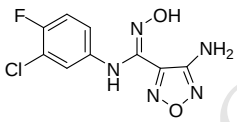	91 ± 2	0.547

[a] IC_{50} values are the mean of five independent assays.
[b] HAC = heavy atom count.
[c] Reported compound

2.3. *Cellular IDO1 inhibitory activities of hydroxyamidines*

To investigate the therapeutic potential of these hydroxyamidines, the ability of the potent compounds in inhibiting the IDO1 activity under the *in vitro* cellular environment

was measured using MDA-MB-231 breast cancer cell line. It is well demonstrated that MDA-MB-231 cells express mRNA of native human IDO1 enzyme and interferon (IFN)-γ considerably induce the IDO1 enzyme expression level in MDA-MB-231 cells [31]. In this regard, MDA-MB-231 cells were first treated with human IFN-γ (20 ng/mL, Fig. S6) for 48 h and then cells were grown in the presence of tested compounds (20, 50, 100 and 500 nM) and *L*-Trp (150μM). The IDO1 activity was determined by measuring the formation of L-kynurenine using the pDMAB-method (Table 4) [27, 28, 31]. The calculated cellular IC_{50} values of most of the tested compounds are in accordance with our *in vitro* enzyme assay data. The calculated IC_{50} values of **1d**, **2i** and **2k** are within 50-71 nM range in MDA-MB-231 cells. Control compound **5l** showed IC_{50} values of 59 nM (Table 4) under the similar experimental conditions [20]. The deviation in IC_{50} values of the compounds between the enzymatic assay against purified IDO1 and cellular assays could be due to the methylene blue-ascorbate regeneration system which maintains IDO1 in active state (Fe^{2+}) or environmental effect on the assay system. In general, a good correlation between these assays confirmed that these tested hydroxyamidine analogues are potent inhibitors of IDO1 enzyme. MTT assay of the compounds (concentrations of IC_{50} and 2 × IC_{50} values from the enzymatic assay) in MDA-MB-231 cells also demonstrated no/negligible level of toxicity of the compounds under the tested conditions (Fig. S7). However, small discrepancy between the IC_{50} values of compounds **2i** and **2k** (as measured by *in vitro* enzymatic and cellular assay) could be also due to the toxicity of the dichloro substituted compound **2k** over difluoro substituted compound **2i** (Fig. S8).

Table 4: IDO1 enzyme inhibitory activity of the selected compounds in MDA-MB-231 cells.

Compound	IDO1 inhibition in MDA-MB-231 cell[a] IC_{50} (nM)[b]
1b	131 ± 17
1d	66 ± 8
1f	242 ± 15
1j	125 ± 17
1n	107 ± 12
2b	131 ± 14
2f	110 ± 19
2h	151 ± 17
2i	50 ± 8
2k	71 ± 10
5l[c]	59 ± 4

[a]IDO protein expression in MDA-MB-231 cells was induced by human IFN-γ (20 ng/mL).
[b]IC_{50} values are the mean of three independent assays.
[c]Reported compound

2.4. *Mode of IDO1 enzyme inhibition by the potent hydroxyamidines*

The enzyme kinetics of selected compounds was performed and their mode of IDO1 inhibition was calculated from the plots of [S]/V against inhibitor concentrations. Four compounds from both the series of hydroxyamidines were selected best on their stronger inhibitory activities against purified IDO1 enzyme. The results showed that compounds **1b, 1n, 2b, 2h, 2i** and **2k** had competitive modes of IDO1 enzyme inhibition whereas compounds **1d, 1f** and **1j** followed uncompetitive modes of IDO1 enzyme inhibition under the similar experimental conditions (Fig. 2 and S9). [S] and V represent the substrate concentration and initial rate of the reaction, respectively [32]. It is important to

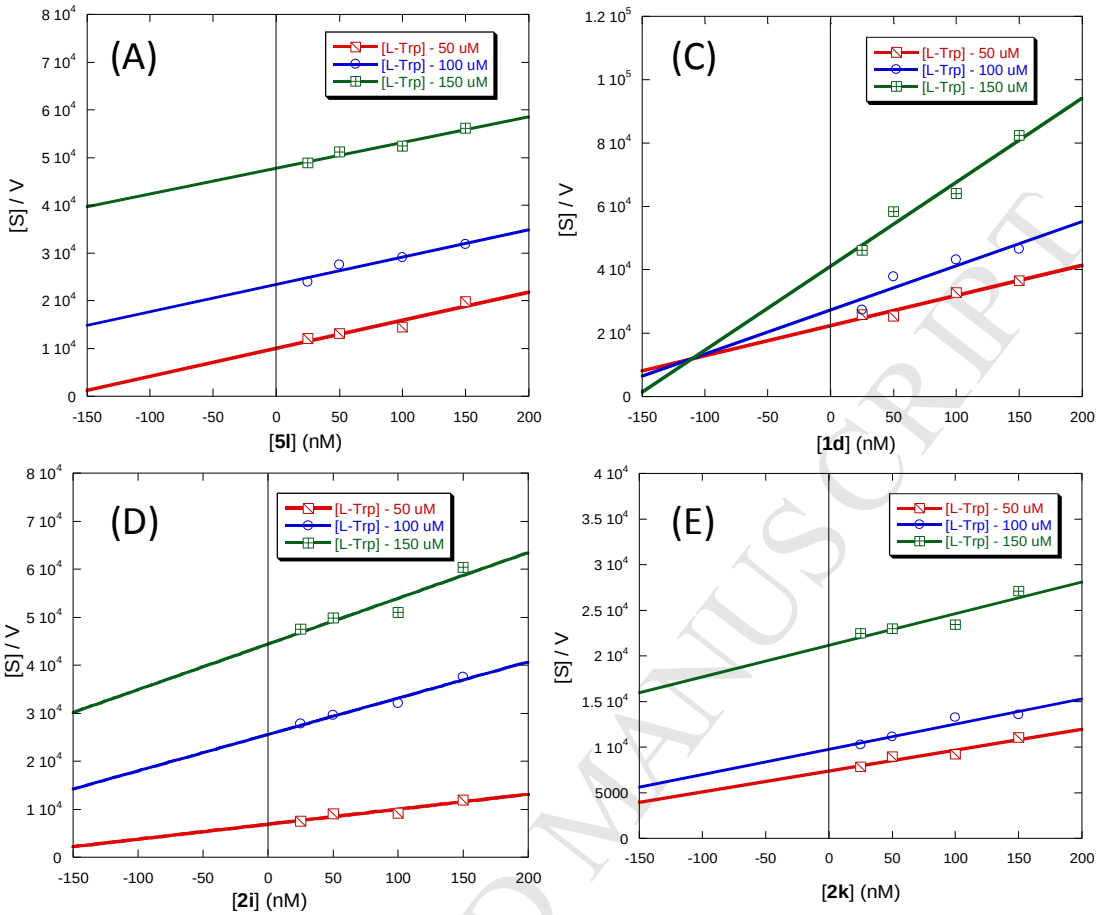

Fig. 2: Determination of mode of inhibition of the potent compounds. Plot of [S]/V against concentrations of compounds **5l** (A), **1d** (B), **2i** (C) and **2k** (D). Concentration of *L*-Trp was varied from 50 to 150 µM. The concentrations of compounds were varied from 25 to 150 nM.

mention that IDO1 is an oxido-reductase enzyme and binding of O_2 to the heme-group is required for the transformation of *L*-Trp to N-formylkynurenine. The results showed that the tested compounds followed competitive or uncompetitive modes of enzyme inhibition with respect to *L*-Trp. However, these compounds may also follow different mode of inhibition with respect to O_2 under the similar experimental conditions. Hence, additional

enzyme kinetics measurement with respect to O_2 is required for detailed understanding, which is beyond the scope of the current study. Compound **5l** is a known competitive inhibitor of hIDO1 enzyme which is in accordance with our experimental results [20].

2.5. *Probable mode of interaction of the potent compounds with IDO1 enzyme*

With confirmation that potent hydroxyamidines strongly inhibit IDO1 enzyme activity, we performed molecular docking analyses to investigate the probable mode of interaction of the potent compounds with the IDO1 enzyme (PDB code: 4PK5) [33]. The docked structures propose that nitrobenzofurazan derivatives of the substituted hydroxyamidines may have different modes of interactions with the IDO1 enzyme (Fig. 3 and S10). Although both the substituted phenyl ring of the *N′*-hydroxy-benzimidamide and *N′*-hydroxy-phenylacetimidamide moieties of the compounds are placed in 'pocket-A' of the IDO1 enzyme, but the *N′*-hydroxy group may interact differently. For analogous of compound **1** the *N′*-hydroxy group interacts with Ser167 residue and pyrrole ring of the heme-group through hydrogen bonding (Fig. S9A-C). Whereas, for analogous of compound **2** the *N′*-hydroxy group interacts with Fe-atom and pyrrole ring of the heme-group. Hydrophobic amino acids like Phe163, Phe164, Tyr126 and others present in 'pocket-A' could be also involved in hydrophobic interaction with the substituted benzene and phenyl groups. A similar mode of interaction was also observed for the reported compounds **5l**, which is accordance with the reported mode of interaction [20]. Therefore, both hydrogen bonding and hydrophobic interactions play important roles in stronger binding of the compounds to the active site of IDO1 enzyme. However, there are no considerable differences in mode of interaction of the compounds from the same

series with the IDO1 enzyme (Fig. 3 and S10). Therefore, in addition to the presence of nitrobenzofurazan and *N*′-hydroxyamidine moieties to the compound's core structure, volume and electronic properties of the substituents in the benzene ring are also crucial for stronger binding to the IDO1 enzyme. These docking analyses also support that substituted hydroxy-2-phenylacetimidamides may act as a mimic of alkylperoxy transition/intermediate state of the transformation of L-Trp to *N*-formylkynurenine by IDO1 enzyme.

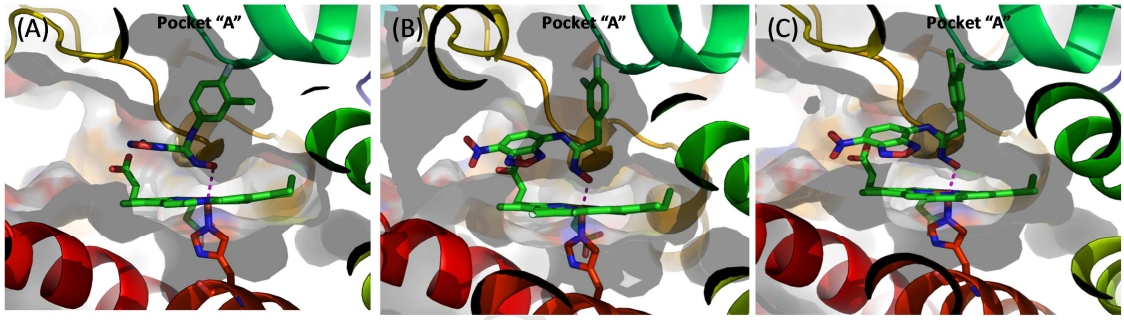

Fig. 3: Predicted mode of interaction of the compounds, **5l** (A), **2i** (B) and **2k** (C) with the active site of the human IDO1 enzyme (4PK5). The modeled structures were generated using MoleGro Virtual Docker (MVD), version 6.0. The oxygen and nitrogen atoms are shown in red and blue, respectively. Residues involved in interactions through hydrogen bond formation are shown using dashed lines (pink color).

2.6. *Inhibitory activities of hydroxyamidines against purified TDO enzyme*

Strong IDO1 inhibition proficiency and very good ligand efficiency (LE > 0.4) of the compounds prompted us to determine their selectivity for IDO1 over TDO enzyme. It is well documented that TDO enzyme is primarily responsible for the catabolism of L-Trp in

liver and maintaining its level through kynurenine pathway. Counter-screening against TDO enzyme showed that the potent compounds were appreciably inactive ($IC_{50} \geq 20$ μM) against TDO enzyme (Table 5). Tested compounds showed 100 to 1700-fold stronger IDO1 inhibition in comparison with TDO enzyme, demonstrating their selectivity for IDO1 enzyme. The most potent compound, **2i** (based on the cellular assay) exhibited over 1550-fold stronger IDO1 inhibitory activity against that of TDO enzyme. HPLC-based TDO activity assay also showed that these potent compounds have preferential selectivity for IDO1 over TDO enzyme inhibitions (Table S2).

Table 5: Inhibitory activity of the selected compounds against purified human IDO1 and TDO enzymes

Compound	Mode of hIDO1 Inhibition	hIDO1 inhibition (IC_{50} (nM))[a]	hTDO inhibition (IC_{50} (μM))[a]	Selectivity ratio[b]
1b	competitive	63 ± 3	110 ± 13	1746
1d	uncompetitive	80 ± 6	25 ± 3	312
1f	uncompetitive	75 ± 5	45 ± 5	600
1h	NM[c]	105 ± 3	20 ± 1	190
1j	uncompetitive	100 ± 9	21 ± 1	210
1k	NM[c]	113 ± 7	40 ± 2	354
1l	NM[c]	117 ± 1	50 ± 7	427
1n	competitive	92 ± 1	47 ± 1	511
2b	competitive	101 ± 5	30 ± 2	297
2f	NM[c]	98 ± 10	51 ± 8	520
2g	NM[c]	127 ± 1	43 ± 2	338
2h	competitive	112 ± 7	65 ± 12	580
2i	competitive	59 ± 5	94 ± 14	1593
2j	NM[c]	160 ± 12	19 ± 1	118
2k	competitive	39 ± 1	32 ± 2	820
5l[d]	competitive	91 ± 2	24 ± 1	263

[a]IC_{50} values are the mean of three independent assays against purified enzymes.
[b]Selectivity ratio is calculated as (IC_{50} value of IDO1)/ (IC_{50} value of TDO).
[c]NM = not measured
[d]Reported compound

In this study nitrobenzofurazan derivatives of the *N′*-hydroxy-benzimidamides and *N′*-hydroxy-phenylacetimidamides were designed as a new class of IDO1 enzyme inhibitors. Suitable substitutions in the benzene ring of the compounds lead to the identification of potent compounds with nanomolar (< 100 nM) IDO1 enzyme inhibitory activities under *in vitro* conditions. The potency of the selected compounds under cellular environment (IC_{50} = 50-242 nM) and no/ negligible level of toxicity at the cellular level reveal the therapeutic potential of the nitrobenzofurazan derivatives of *N′*-hydroxyamidines. Measured IC_{50} values and molecular modeling studies of the compounds suggest that the presence of hydroxyamidine and nitrobenzofurazan moieties and suitable substitution in the benzene ring of the compounds play a critical role in their stronger IDO1 enzyme inhibitory properties. Until now, only few hydroxyamidine based compounds have been reported with such stronger IDO1 enzyme inhibition properties [20]. The inhibition modes of the tested compounds were determined to be both either competitive or uncompetitive. The potent hydroxyamidine analogues also showed 100 to 1700-fold stronger IDO1 enzyme inhibitory activities in comparison with TDO enzyme, which catabolizes L-Trp through the same mechanistic pathway. The low cytotoxicity and inactivity for TDO enzyme support further development of nitrobenzofurazan derivatives of hydroxyamidines.

3. Conclusion

In this study, we synthesized a new series of nitrobenzofurazan derivatives of *N′*-hydroxyamidines. Most of the tested compounds showed strong inhibitory activities against purified IDO1 enzyme. The presence of both *N′*-hydroxyamidine and

nitrobenzofurazan moieties in the compound's core structure could be the driving force for their strong inhibitory activities. Halogen substitutions in the aryl ring were successful in improving the potency. IDO1 inhibition assay in the interferon-γ-induced MBA-MB-231 cells showed that the nitrobenzofurazan derivatives of hydroxyamidines **1d**, **2i** and **2k** have minimal toxicity and stronger potencies. These hydroxyamidine derivatives also exhibited stronger selectivity for IDO1 enzyme over TDO enzyme. These compounds also could be considered as good molecular probes on the basis of their ligand efficiency values. Overall, our findings suggest that these nitrobenzofurazan derivatives of the *N′*-hydroxyamidines can be a useful structural class of compounds for cancer and other human diseases.

4. Experimental section

4.1. *General information*

All reagents were purchased from different commercial sources and used directly without further purification. Column chromatography was performed using 60―120 mesh silica gel. Reactions were monitored by thin-layer chromatography (TLC) on silica gel 60 F254 (0.25 mm). ^{1}H NMR and ^{13}C NMR were recorded at 400 and 100 MHz respectively, with Varian AS400 spectrometer and 600 and 151 MHz respectively, with Brucker spectrometer, using TMS as an internal standard with $CDCl_3$ and DMSO-d_6. The coupling constant (J values) and chemical shifts (δ_{ppm}) were described in Hertz (Hz) and parts per million (ppm) respectively. Multiplicities are described as follows: s (singlet), d (doublet), t (triplet), m (multiplet) and br (broadened). High resolution mass spectra

(HRMS) were recorded at Agilent Q-TOF mass spectrometer with Z-spray source using built-in software for analysis of the recorded data.

4.2. *General procedure for the synthesis of substituted hydroxyamidines*

To a stirring solution of substituted benzonitrile/ phenylacetonitrile (1 mmol) in anhydrous methanol (20 mL) under N_2 atmosphere was added hydroxylamine hydrochloride (1.2 mmol). Triethylamine (2.5 mmol) was added under continuous stirring condition and the mixture was then heated under reflux condition for overnight at 60 °C and continued until complete consumption of the starting material (monitored by TLC) [22, 23]. The excess solvent was then removed under reduced pressure and the obtained residue was washed successively with water and brine, and extracted with ethylacetate (3 × 10 mL).The organic layer was dried over anhydrous Na_2SO_4 and concentrated under reduced pressure. This reaction mixture was purified using silica gel column chromatography with a gradient solvent system of 10-20% ethylacetate to hexane to obtain the desired product with an average yield of 70-80%.

4.3. *General procedure for the synthesis of 2-substituted N'-hydroxy, N- (7 nitro benzoxadiazole) imidamide*

Sodium bicarbonate (3.5 mmol) was added to a stirring solution of 2-substituted *N'*-hydroxyimidamide (1.1 mmol) in 20 ml of EtOH/H_2O (9:1) and the solution was stirred for 10 min at room temperature. To this mixture an ethanolic solution of 4-chloro 7-nitrobenzofurazan (1 mmol) was added drop wise under continuous stirring condition and the resulting solution was stirred at 50 °C for another 2-4 hours [24]. After completion of

the reaction (monitored by TLC) the excess solvent was removed under reduced pressure and the pH adjusted to 1.5 using 1N HCl solution. Then aqueous layer was extracted with dichloromethane (3 × 20 ml) and the organic layer was dried over anhydrous Na_2SO_4 and concentrated under reduced pressure. The reaction mixture was further purified using silica gel column chromatography using 20-30% ethylacetate to hexane gradient solvent system to afford the desired pure product with 60-90% yield.

4.4. *Characterization of the synthesized compounds*

(Z)-N'-hydroxy-N-(7-nitrobenzo[c][1,2,5]oxadiazol-4-yl)benzimidamide (1a): As yellow solid (85 % yield; mp: 201-203 °C); ^{1}H NMR (600MHz, $CDCl_3$ + DMSO-d_6) δ_{ppm} 8.50 (d, 1H, J = 12 Hz), 7.70 (d, 1H, J = 12 Hz), 7.46-7.36 (m, 5H), 6.12 (br s, 1H);^{13}C NMR (151 MHz, $CDCl_3$ + DMSO-d_6) δ_{ppm} 157.7, 154.3, 144.1, 144.0, 134.9, 131.5, 130.6, 129.2, 128.9, 126.9, 106.7; HRMS (ESI) calcd. for $C_{13}H_9N_5O_4$ $[M + H]^+$ 300.0727, found 300.0725.

(Z)-2-fluoro-N'-hydroxy-N-(7-nitrobenzo[c][1,2,5]oxadiazol-4-yl)benzimidamide (1b): As yellow solid (60 % yield; mp: 134-135 °C); ^{1}H NMR (400MHz, DMSO-d_6) δ_{ppm} 8.55 (d, 1H, J = 8.8 Hz), 7.64-7.62 (m, 1H), 7.47-7.45 (m, 1H), 7.37 (d, 1H, J = 8.4 Hz), 7.23-7.13 (m, 2H), 6.74 (br, s, 1H); ^{13}C NMR (151 MHz, $CDCl_3$+DMSO-d_6) δ_{ppm} 160.7, 154.2, 153.5, 143.2, 143.1, 134.6, 131.8, 129.7, 128.0, 123.6, 115.7, 115.4, 106.1; HRMS (ESI) calcd. for $C_{13}H_8FN_5O_4$ $[M + H]^+$ 318.0633, found 318.0635.

(Z)-2-chloro-N'-hydroxy-N-(7-nitrobenzo[c][1,2,5]oxadiazol-4-yl)benzimidamide (1c): As yellow solid (70 % yield; mp: 178-180 °C); ^{1}H NMR (600MHz, $CDCl_3$ + DMSO-d_6) δ_{ppm} 8.45 (d, 1H, J = 12 Hz), 7.48-7.46 (m, 1H), 7.40-7.35 (m, 2H), 7.32-7.27 (m, 2H), 6.24 (br s, 1H); ^{13}C NMR (151 MHz, $CDCl_3$ + DMSO-d_6) δ_{ppm} 161.3, 158.5, 148.0, 147.9, 139.5, 139.3, 136.9, 135.6, 134.8, 134.7, 132.8, 131.0, 110.9; HRMS (ESI) calcd. for $C_{13}H_8ClN_5O_4$ $[M + H]^+$ 334.0338, found 334.0340.

(Z)-2-bromo-N'-hydroxy-N-(7-nitrobenzo[c][1,2,5]oxadiazol-4-yl)benzimidamide (1d): As brown solid (60 % yield; mp: 162-164 °C); ^{1}H NMR (400MHz, $CDCl_3$ + DMSO-d_6) δ_{ppm} 8.50 (d, 1H, J = 8.4 Hz), 7.61 (d, 1H, J = 7.6 Hz), 7.49-7.42 (m, 1H), 7.37-7.29 (m, 3H), 6.53 (br, s, 1H); ^{13}C NMR (151 MHz, $CDCl_3$ + DMSO-d_6) δ_{ppm} 157.8, 154.0, 143.7, 143.5, 134.9, 133.0, 132.2, 131.4, 130.8, 128.5, 127.2, 121.7, 106.5; HRMS (ESI) calcd. for $C_{13}H_8BrN_5O_4$ $[M + H]^+$ 377.9832, found 377.9835.

(Z)-N'-hydroxy-3-methyl-N-(7-nitrobenzo[c][1,2,5]oxadiazol-4-yl)benzimidamide (1e): As yellow solid (75 % yield; mp: 203-205 °C); ^{1}H NMR (400MHz, $CDCl_3$ + DMSO-d_6) δ_{ppm} 8.38-8.35 (m, 1H), 7.58-7.56 (m, 1H),7.30-7.21 (m, 4H), 6.18 (br, s, 1H), 2.29 (s, 3H); ^{13}C NMR (151 MHz, $CDCl_3$ + DMSO-d_6) δ_{ppm} 157.8, 154.6, 144.2, 135.1, 132.3, 131.3, 130.6, 128.7, 126.9, 106.7, 22.8; HRMS (ESI) calcd. for $C_{14}H_{11}N_5O_4$ $[M + H]^+$ 314.0884, found 314.0880.

(Z)-3-fluoro-N'-hydroxy-N-(7-nitrobenzo[c][1,2,5]oxadiazol-4-yl)benzimidamide (1f): As yellow solid (75 % yield; mp: 167-169 °C); ^{1}H NMR (600MHz, $CDCl_3$ + DMSO-d_6) δ_{ppm}

8.54-8.51 (m, 1H), 7.75-7.72 (m, 1H), 7.47-7.39 (m, 3H), 7.35-7.34 (m, 1H), 6.23 (br, s, 1H); ^{13}C NMR (151 MHz, $CDCl_3$ + DMSO-d_6) δ_{ppm} 157.7, 154.3, 143.9, 143.7, 135.0, 131.1, 130.5, 128.8, 128.6, 126.8, 106.5; HRMS (ESI) calcd. for $C_{13}H_8FN_5O_4$ $[M + H]^+$ 318.0633, found 318.0635.

(Z)-3-chloro-N'-hydroxy-N-(7-nitrobenzo[c][1,2,5]oxadiazol-4-yl)benzimidamide (1g): As yellow solid (77 % yield; mp: 210-212 °C);^{1}H NMR (400MHz, $CDCl_3$ + DMSO-d_6) δ_{ppm} 8.64 (d, 1H, J = 8.8 Hz), 7.87 (s, 1H), 7.77 (d, 1H, J = 7.6 Hz), 7.53-7.51 (m, 2H), 7.47-7.43 (m, 1H), 6.72 (br, s, 1H); ^{13}C NMR (100 MHz, $CDCl_3$ + DMSO-d_6) δ_{ppm} 156.2, 153.8, 143.6, 143.4, 134.8, 133.9, 132.0, 130.6, 129.5, 128.5, 126.7, 124.8, 106.3; HRMS (ESI) calcd. for $C_{13}H_8ClN_5O_4$ $[M + H]^+$ 334.0338, found 334.0340.

(Z)-3-bromo-N'-hydroxy-N-(7-nitrobenzo[c][1,2,5]oxadiazol-4-yl)benzimidamide (1h): As yellow solid (78 % yield; mp: 189-191 °C); ^{1}H NMR (400MHz, $CDCl_3$ + DMSO-d_6) δ_{ppm} 8.53-8.49 (m, 1H), 7.90-7.87 (m, 1H), 7.69-7.65 (m, 1H), 7.56-7.52(m, 1H),7.42-7.40 (m, 1H), 7.29-7.24 (m, 1H), 6.40 (br, s, 1H); ^{13}C NMR (151 MHz, $CDCl_3$ + DMSO-d_6) δ_{ppm} 156.3, 154.0, 134.8, 133.9, 132.5, 130.1, 129.8, 125.5, 106.5; HRMS (ESI) calcd. for $C_{13}H_8BrN_5O_4$ $[M + H]^+$ 377.9832, found 377.9828.

(Z)-N'-hydroxy-4-methyl-N-(7-nitrobenzo[c][1,2,5]oxadiazol-4-yl)benzimidamide (1i): As yellow semi solid (70 % yield); ^{1}H NMR (600MHz, $CDCl_3$ + DMSO-d_6) δ_{ppm} 8.65 (d, 1H, J = 12 Hz), 7.71 (d, 2H, J = 12 Hz), 7.57 (d, 1H, J = 12 Hz), 7.37 (d, 2H, J = 12 Hz),

1.31 (s, 3H); ^{13}C NMR (151 MHz, $CDCl_3$ + DMSO-d_6) δ_{ppm}157.5, 154.2, 143.8, 143.6, 140.7, 135.8, 128.8, 128.1, 127.5, 126.6, 106.7, 21.0; HRMS (ESI) calcd. for $C_{14}H_{11}N_5O_4$ $[M + H]^+$ 314.0884, found 314.0882.

(Z)-4-fluoro-N'-hydroxy-N-(7-nitrobenzo[c][1,2,5]oxadiazol-4-yl)benzimidamide (1j): As yellow solid (70 % yield; mp: 191-193 °C); ^{1}H NMR (600MHz, $CDCl_3$) δ_{ppm} 8.58 (d, 1H, *J* = 8.4 Hz), 7.79-7.76 (m, 2H),7.49 (d, 1H, *J* = 8.4 Hz), 7.22-7.19 (m, 2H), 5.49 (br, s, 1H);^{13}C NMR (151 MHz, $CDCl_3$) δ_{ppm} 156.5, 154.1, 144.0, 134.8, 129.1, 129.0, 116.6, 116.5, 106.9; HRMS (ESI) calcd. for $C_{13}H_8FN_5O_4$ $[M + H]^+$318.0633, found 318.0635.

(Z)-4-chloro-N'-hydroxy-N-(7-nitrobenzo[c][1,2,5]oxadiazol-4-yl)benzimidamide (1k): As orange solid (50 % yield; mp: 200-202 °C); ^{1}H NMR (600MHz, $CDCl_3$ + MeOD-d_4+ DMSO-d_6) δ_{ppm} 8.56 -8.54 (m, 1H), 7.74-7.72 (m, 2H), 7.44-7.41 (m, 1H), 7.38-7.36 (m, 2H), 6.68 (br, s, 1H); ^{13}C NMR (151 MHz, $CDCl_3$ + MeOD-d_4 + DMSO-d_6) δ_{ppm} 156.8, 154.2, 144.0, 143.8, 136.8, 135.3, 129.1, 128.7, 128.3, 106.7; HRMS (ESI) calcd. for $C_{13}H_8ClN_5O_4$ $[M + H]^+$334.0338, found 334.0338.

(Z)-4-bromo-N'-hydroxy-N-(7-nitrobenzo[c][1,2,5]oxadiazol-4-yl)benzimidamide (1l): As orange solid (65 % yield; mp: 213-215 °C); ^{1}H NMR (400MHz, $CDCl_3$ + DMSO-d_6) δ_{ppm} 8.61-8.59 (m, 1H), 7.73-7.71 (m, 2H), 7.56-7.54 (m, 2H), 7.44-7.42 (m, 1H), 6.98 (br, s, 1H); ^{13}C NMR (100 MHz, $CDCl_3$ + DMSO-d_6) δ_{ppm} 156.6, 154.0, 143.7, 143.5, 135.4, 131.3, 129.5, 128.5, 128.3, 124.7, 106.6; HRMS (ESI) calcd. for $C_{13}H_8BrN_5O_4$ $[M + H]^+$ 379.9813, found 379.9848.

(Z)-3-chloro-4-fluoro-N'-hydroxy-N-(7-nitrobenzo[c][1,2,5]oxadiazol-4-yl)benzimidamide (1m): As yellow solid (50 % yield; mp: 251-253 °C); ^{1}H NMR (600MHz, MeOD-d_4) δ_{ppm} 8.43 (d, 2H, J = 8 Hz), 7.42 (s, 1H), 6.08 (d, 2H, J = 8 Hz); ^{13}C NMR (151 MHz, MeOD-*d4*+ DMSO-d_6) δ_{ppm} 148.5, 146.5, 139.3, 114.7, 112.1; HRMS (ESI) calcd. for $C_{13}H_7ClFN_5O_4$ $[M + H]^+$ 351.0171 found 351.0168.

(Z)-3-bromo-4-fluoro-N'-hydroxy-N-(7-nitrobenzo[c][1,2,5]oxadiazol-4-yl)benzimidamide (1n): As brown solid (60 %; yield; mp: 112-113 °C); ^{1}H NMR (600MHz, $CDCl_3$ + DMSO-d_6) δ_{ppm} 8.55 (d, 1H, J = 12 Hz), 8.03-8.01 (m, 1H), 7.95 (s, 1H), 7.75-7.71 (m, 1H), 7.44 (d, 1H, J = 12 Hz), 7.21-7.17 (m, 1H), 6.20 (br s, 1H); ^{13}C NMR (100 MHz, MeOD-d_4 + $CDCl_3$ + DMSO-d_6) δ_{ppm} 160.9, 159.2, 155.5, 153.7, 143.5, 143.4, 134.9, 131.7, 128.4, 127.9, 116.2, 116.0, 106.3; HRMS (ESI) calcd. for $C_{13}H_7BrFN_5O_4$ $[M + H]^+$ 397.9719, found 397.9752 .

(Z)-N'-hydroxy-N-(7-nitrobenzo[c][1,2,5]oxadiazol-4-yl)-2-phenylacetimidamide (2a): As red semi solid (90% yield); ^{1}H NMR (400MHz, $CDCl_3$ + DMSO-d_6) δ_{ppm}8.59 (d, 1H, J = 8 Hz), 7.45 (d, 1H, J = 8 Hz), 7.41-7.34 (m, 5H), 5.10 (br, s, 1H), 3.66 (s, 2H);^{13}C NMR (151 MHz, $CDCl_3$ + DMSO-d_6) δ_{ppm} 158.5, 154.4, 144.2, 144.0, 135.1, 134.9, 129.2, 129.0, 127.8, 106.7, 37.2; HRMS (ESI) calcd. for $C_{14}H_{11}N_5O_4$ $[M + H]^+$ 314.0884, found 314.0909.

(Z)-2-(2-fluorophenyl)-N'-hydroxy-N-(7-nitrobenzo[c][1,2,5]oxadiazol-4-yl)acetimidamide (2b): As yellow solid (85 % yield; mp:148-150 °C);^{1}H NMR (600MHz, $CDCl_3$ + DMSO-d_6) δ_{ppm} 8.48-8.45 (m, 1H), 7.29-7.25 (m, 2H), 7.20-7.18 (m, 1H), 7.06-7.04 (m, 1H), 7.01-6.99 (m, 1H), 5.69 (br, s, 1H), 3.57 (s, 2H); ^{13}C NMR (100 MHz, $CDCl_3$ + DMSO-d_6) δ_{ppm} 157.9, 154.4, 144.2, 144.0, 135.2, 131.1, 129.6, 129.6, 127.2, 124.8, 119.7, 115.6, 106.6, 30.5; HRMS (ESI) calcd. for $C_{14}H_{10}FN_5O_4$ $[M + H]^+$ 332.0790, found 332.0789.

(Z)-2-(3-fluorophenyl)-N'-hydroxy-N-(7-nitrobenzo[c][1,2,5]oxadiazol-4-yl)acetimidamide (2c): As yellow solid (70 % yield; mp:140-142 °C);^{1}H NMR (600MHz, $CDCl_3$ + DMSO-d_6) δ_{ppm}8.61-8.54 (m, 1H), 7.38-7.31 (m, 3H), 7.20-6.93 (m, 2H), 5.84 (s, 1H), 3.55 (s, 2H); ^{13}C NMR (151 MHz, $CDCl_3$ + DMSO-d_6) δ_{ppm}163.9, 162.3, 158.3, 154.5, 144.2, 144.0, 137.8, 135.2, 130.5, 124.7, 116.1, 114.6, 106.6, 36.9; HRMS (ESI) calcd. for $C_{14}H_{10}FN_5O_4$ $[M + H]^+$ 332.0790, found 332.0791.

(Z)-2-(3-chlorophenyl)-N'-hydroxy-N-(7-nitrobenzo[c][1,2,5]oxadiazol-4-yl)acetimidamide (2d): As orange solid (87% yield; mp: 152-154 °C); ^{1}H NMR (400MHz, $CDCl_3$ + DMSO-d_6) δ_{ppm} 8.59 (d, 1H, J = 8 Hz), 7.44 (d, 1H, J = 8 Hz), 7.36-7.32 (m, 3H), 7.26-7.24 (m, 1H), 5.14 (br, s, 1H), 3.64 (s, 2H);^{13}C NMR (151 MHz, $CDCl_3$ + DMSO-d_6) δ_{ppm} 158.0, 154.0, 143.5, 143.4, 137.3, 134.8, 129.5, 128.4, 126.8, 126.6, 106.0, 36.1; HRMS (ESI) calcd. for $C_{14}H_{10}ClN_5O_4$ $[M + H]^+$348.0494, found 348.0525 .

(Z)-N'-hydroxy-2-(4-methoxyphenyl)-N-(7-nitrobenzo[c][1,2,5]oxadiazol-4-yl)acetimidamide (2e): As orange solid (80 % yield; mp: 166-168 °C); ^{1}H NMR (400MHz, $CDCl_3$ + DMSO-d_6) δ_{ppm} 8.59 (d, 1H, J = 8 Hz), 7.45 (d, 1H, J = 8 Hz), 7.29-7.24 (m, 2H), 6.92 (d, 2H, J = 8 Hz), 3.82 (s, 3H), 3.59 (s, 2H);^{13}C NMR (151 MHz, $CDCl_3$ + DMSO-d_6) δ_{ppm} 158.8, 154.3, 143.8, 143.7, 135.0, 129.7, 126.8, 114.0, 106.3, 55.1, 36.0; HRMS (ESI) calcd. for $C_{15}H_{13}N_5O_5$ $[M + H]^+$ 344.0989, found 344.1020 .

(Z)-2-(4-chlorophenyl)-N'-hydroxy-N-(7-nitrobenzo[c][1,2,5]oxadiazol-4-yl)acetimidamide (2f): As yellow solid (85% yield; mp: 163-165 °C); ^{1}H NMR (400MHz, $CDCl_3$ + DMSO-d_6) δ_{ppm} 8.59 (d, 1H, J = 8 Hz), 7.43 (d, 1H, J = 8 Hz), 7.38-7.36 (m, 2H), 7.30-7.28 (m, 2H), 5.12 (br, s, 1H), 3.63 (s, 2H);^{13}C NMR (151 MHz, $CDCl_3$ + DMSO-d_6) δ_{ppm} 158.2, 154.1, 143.6, 143.4, 134.8, 133.7, 132.5, 129.9, 128.3, 106.1, 35.9; HRMS (ESI) calcd. for $C_{14}H_{10}ClN_5O_4$ $[M + H]^+$ 348.0494, found 348.0521.

(Z)-2-(4-bromophenyl)-N'-hydroxy-N-(7-nitrobenzo[c][1,2,5]oxadiazol-4-yl)acetimidamide (2g): As brown solid (75 % yield; mp: 185-187 °C);^{1}H NMR (600MHz, MeOD-d_4 + $CDCl_3$ + DMSO-d_6) δ_{ppm} 8.70 (d, 1H, J = 9 Hz), 7.52 (d, 2H, J = 8.4 Hz), 7.43 (d, 1H, J = 8.4 Hz), 7.36 (d, 2H, J = 8.4 Hz), 3.55 (s, 2H); ^{13}C NMR (100 MHz, $CDCl_3$ + DMSO-d_6) δ_{ppm} 161.6, 155.6, 145.4, 136.6, 132.6, 132.4, 131.6, 128.7, 126.9, 117.4, 112.3, 107.4, 37.1; HRMS (ESI) calcd. for $C_{14}H_{10}BrN_5O_4$[M + H]$^+$ 391.9989, found 391.9989 .

(Z)-2-(4-fluorophenyl)-N'-hydroxy-N-(7-nitrobenzo[c][1,2,5]oxadiazol-4-yl)acetimidamide (2h): As yellow solid (85 % yield; mp: 170-172 °C); ^{1}H NMR (600MHz, $CDCl_3$ + DMSO-d_6) δ_{ppm} 8.43 (d, 1H, J = 12 Hz), 7.26-7.18 (m, 3H), 6.89-6.85 (m, 2H), 5.81 (br, s, 1H), 3.42 (s, 2H); ^{13}C NMR (100 MHz, $CDCl_3$ + DMSO-d_6) δ_{ppm} 162.8, 160.3, 158.5, 154.1, 143.6, 143.5, 135.0, 130.9, 130.1, 130.1, 128.2, 115.2, 106.1, 35.8; HRMS (ESI) calcd. for $C_{14}H_{10}FN_5O_4$ $[M + H]^+$ 332.0790, found 332.0789 .

(Z)-2-(3,4-difluorophenyl)-N'-hydroxy-N-(7-nitrobenzo[c][1,2,5]oxadiazol-4-yl)acetimidamide (2i): As yellow solid (65% yield; mp: 165-167 °C); ^{1}H NMR (600MHz, $CDCl_3$ + DMSO-d_6) δ_{ppm} 8.30-8.26 (m, 1H), 7.13-7.06 (m, 2H), 6.96-6.93 (m, 1H), 6.82 (s, 1H), 5.86 (br s, 1H), 3.25 (s, 2H); ^{13}C NMR (151 MHz, $CDCl_3$ + DMSO-d_6) δ_{ppm} 158.1, 154.2, 143.9, 143.7, 135.0, 132.3, 128.7, 124.9, 117.8, 117.7, 117.3, 117.2, 106.4, 36.1; HRMS (ESI) calcd. for $C_{14}H_9F_2N_5O_4$ $[M + H]^+$ 350.0695, found 350.0695.

(Z)-2-(2,4-difluorophenyl)-N'-hydroxy-N-(7-nitrobenzo[c][1,2,5]oxadiazol-4-yl)acetimidamide (2j): As yellow solid (70 % yield; mp: 174-176 °C); ^{1}H NMR (600MHz, $CDCl_3$ + DMSO-d_6) δ_{ppm} 8.59-8.58(m, 1H), 7.39-7.35 (m, 3H), 6.91-6.87 (m, 1H), 5.87 (br, s, 1H), 3.65 (s, 2H); ^{13}C NMR (151 MHz, $CDCl_3$ + DMSO-d_6) δ_{ppm} 157.5, 154.2, 144.0, 143.8, 135.0, 131.7, 128.9, 120.7, 111.8, 106.5, 103.8, 29.8; HRMS (ESI) calcd. for $C_{14}H_9F_2N_5O_4$ $[M + H]^+$ 350.0695, found 350.0692.

(Z)-2-(3,4-dichlorophenyl)-N'-hydroxy-N-(7-nitrobenzo[c][1,2,5]oxadiazol-4-yl)acetimidamide (2k): As yellow solid (88 % yield; mp: 183-185 °C); ^{1}H NMR

(600MHz, $CDCl_3$ + DMSO-d_6) δ_{ppm} 8.98 (d, 1H, J = 6 Hz), 7.87 (s, 1H), 7.83 (d, 1H, J = 6 Hz), 7.79 (d, 1H, J = 12 Hz), 7.61-7.60 (m, 1H), 6.04 (br s, 1H), 3.97 (s, 2H); ^{13}C NMR (100 MHz, $CDCl_3$ + DMSO-d_6) δ_{ppm} 157.9, 154.2, 143.9, 143.7, 135.7, 135.0, 132.4, 131.2, 130.8, 130.5, 128.8, 128.3, 106.4, 36.1; HRMS (ESI) calcd. for $C_{14}H_9Cl_2N_5O_4$ [M + H]$^+$ 382.0104, found 382.0113.

4.5. *Purification of the compounds by HPLC analysis*

All compounds were further purified by analytical-HPLC analyses (with a purity level ≥ 94-95 %) and used for enzymatic assay, cellular activity assay, MTT assay, morphological analysis and others. The compounds were purified using Varian star # 1 HPLC system with a Hypersil GOLD aQ C18 analytical column (Thermo Scientific) at a flow rate of 1mL/min. All the compounds (~1mg) were dissolved in MeOH (1mL) for HPLC analyses. All the compounds have a strong absorption peak at 465 nm. In this regard, HPLC analyses were performed using a UV-detector at 465 nm. During each injection 20 µL of the compound solution was used and fractions were collected. This step was repeated for more than 10-times to get sufficient amount of the pure compounds. A total run time was 10 min. All the collected fractions for each compound were dried under reduced pressure and verified by HRMS analyses. The mobile phase for HPLC measurements was 60% MeOH & 40% H_2O (isocratic mode).

4.6. *Expression and purification of human IDO1 enzyme*

The cDNA of human IDO1 (in the vector pQE30) with an N-terminus hexa-histidyl tag was used for the current study. The cDNA was a generous gift from Professor Emma

Raven (University of Leicester). The pQE30-IDO1 and pREP4 plasmids were transformed in *E. coli*-M15 cells and used for over-expression of IDO1 enzyme [27]. The cells were grown at 37 °C to an OD_{600} of 0.6 in Luria-Bertani (LB) medium containing 100 μg/mL of ampicillin and 50 μg/mL of kanamycin. After cooling down the flask in an ice/water bath, the protein expression was induced by the addition of 5-aminolevulinic acid (0.5 mM), IPTG (1 mM) and PMSF (1 mM). The cells were then grown at 30 °C for 24 h. The flask was then cooled down and cells were collected by centrifugation at 5000 rpm for 10 min (at 4 °C). The cell pellet was then re-suspended in 20 mL of PBS buffer containing 1 mM PMSF and 1 mM ethylenediaminetetraacetic acid (EDTA) and centrifuged at 15000 rpm for 10 min at 4 °C. The cell pellet was stored at -80 °C. After thawing, the cell pellet was collected by centrifugation at 15000 rpm for 10 min at 4 °C. To remove EDTA, cells were again resuspended in 20 mL of 25 mM Tris-buffer at pH 7.4 containing 150 mM NaCl, 10 mM imidazole and 10 mM $MgCl_2$ and 1 mM PMSF. The cell-suspension was then centrifuged at 5000 rpm for 10 min at 4 °C. This washed cell pellet was resuspended in 25 mM Tris buffer at pH 7.4 (20 mL) containing 150 mM NaCl, 10 mM imidazole and 10 mM $MgCl_2$, protease inhibitors (complete EDTA free) and DNase (< 1 mg). The suspension was sonicated on ice using an ultrasonic processor UP100H (Hielscher GmbH) for 10 min (30 s of sonication followed by 30 s of cooling) at maximum power. The cell debris was removed by centrifugation (at 20000 rpm for 30 min) and filtration on 0.22 μm filter.

To the supernatant 1 mL of nickel-nitrilotriacetic acid resin (Qiagen) was added and the mixture was incubated on ice with gentle stirring (80 rpm) for 1 h. After that the mixture was poured onto a column filled with 20 mL of 25 mM Tris buffer at pH 7.4 containing

150 mM NaCl, 10 mM imidazole. After sequentially washing the nonspecifically bound protein with 50 ml of 25 mM Tris buffer at pH 7.4, 150 mM NaCl containing 30, 40, 50, 65 and 80 mM imidazole, respectively, the protein was eluted in five fractions using 25 mM Tris buffer at pH 7.4 containing 150 mM NaCl, 190 mM imidazole. 2 mL of the collected protein was then buffer exchanged into 50 mM Tris, pH 7.4, using a Sephadex-G25 column. Coomassie-blue stained SDS-PAGE gel image of the purified enzyme showed > 90% purity. The absorbance of the purified enzyme was also tested and the ratio of λ_{404} and λ_{280} was around 1.4.

4.7. *IDO1 inhibition assay by spectrophotometric technique*

The IDO1 activity assay was performed (in 500 μL volume) according to the reported procedures [25, 27, 28] in 100 mM potassium phosphate buffer at pH 6.5 using sodium-ascorbate (20 mM), catalase (240 nM), methylene blue (10 μM), purified recombinant IDO1 (41 nM), *L*-Trp (100 μM), DMSO (0.05%, v/v) and triton-X 100 (0.01%, v/v). The concentrations of inhibitors were varied from 50 nM to 1 μM. The reaction mixture was incubated at 37 °C for 1 h and then quenched by addition of 30% (w/v) trichloroacetic acid (100 μL). The reaction mixture was then incubated at 50 °C for 30 minutes and centrifuged at 10000 rpm for 10 minutes. To the supernatant of 100 μL, 2% pDMAB in acetic acid was added and stored for 10 minutes. The amount of kynurenine generated during reactions was indirectly monitored by measuring absorbance at 480 nm, which correspond to the product of kynurenine and pDMAB. A standard curve was prepared with pure kynurenine (from Sigma) under similar experimental conditions [28]. The IC_{50} values were calculated using this standard curve.

4.8. *IDO1 inhibition assay by HPLC analysis*

The enzymatic reaction was carried out (100 μL) in 100 mM potassium phosphate buffer at pH 6.5 using sodium-ascorbate (20 mM), catalase (240 nM), methylene blue (10 μM), purified recombinant IDO1 (41 nM), *L*-Trp (150 μM), DMSO (0.05%, v/v) and triton-X 100 (0.01%, v/v). Inhibitor concentrations of 50 nM and 100 nM were used for this assay. The reaction mixture was incubated at 37 °C in dark for 1 h and then quenched by addition of 30% (w/v) trichloroacetic acid (20 μL).The reaction mixture was further incubated at 50 °C for 30 minutes and then centrifuged at 10000 rpm for 10 minutes. A 20 μL of supernatant from each reaction mixture was used for HPLC analyses. The mobile phase for HPLC measurements was 50% sodium citrate buffer (40 mM, pH 2.25) and 50% methanol with 400 μM SDS. The rate of flow through the Ascentis® Express C18, 2.7μm HPLC column was 0.5 mL/min, and kynurenine was detected at a wavelength of 365 nm [28]. A similar HPLC analyses were performed using pure kynurenine and a standard curve was prepared. The IC_{50} values of the compounds were calculated from this standard curve.

4.9. *Determination of inhibition modes*

The mode of IDO1 enzyme inhibition by the selected compounds was measured according to the reported method [32]. The IDO1 activity assay was performed with 50, 100 and 150 μM of L-tryptophan and 25, 50, 100 and 150 nM of inhibitors. The amount of generated *N*-formylkynurenine was monitored at different time interval by UV-Vis spectroscopy. The mode of inhibition was determined from the plot of [S]/V against

inhibitor concentration [I]. Where, [S] and V represent L-tryptophan concentration and initial rate of enzyme catalysis, respectively [32].

4.10. *In-silico molecular docking analysis*

Molecular docking studies to understand the probable mode of interaction of the compounds with hIDO1 enzyme (PDB code: 4PK5) was performed using MoleGro Virtual Docker version 6.0 (Molegro ApS, Aarhus, Denmark) [33, 34]. To generate apoprotein, the ligands were removed from the co-crystal structures and then were processed by energy minimization. The energy minimized three-dimensional structure of the ligands was prepared by using the GlycoBioChem PRODRG2 server (http://davapc1.bioch.dundee.ac.uk/prodrg/). The occupied position of the ligand PIM (in the crystal structure) was used as the center of docking site (radius: 10 Å; and center: x = -25, y = 51, z = 18). Other parameters were set default during docking analyses. In each docking run, two hundred docked structures were generated for an individual ligand. Energetically favored docked conformations were evaluated on the basis of the moledock and re-rank scores (docking score-based on energy function such as a force field with repulsive and attractive Van-der-Waals terms and an electrostatic term). The docking poses were exported and examined using PyMOL software (The PyMol Molecular Graphics System, Version 1.0r1, Schrödinger, LLC).

4.11. *Cellular activity assay*

MDA-MB-231 breast cancer cells were chosen for the *in vitro* cellular assay. 50,000 cells were seeded in each well of a 24-well plate in DMEM F12 complete media and were

allowed to adhere overnight. First, cells were treated with different concentration of human IFN-γ (from 5-1000 ng/mL) in complete media for a period of 48 h. Following this, 150 μM tryptophan was added and treated for additional period of 5 h. Post treatment phase, the cells were washed with sterile cell-culture grade PBS and were trypsinized and centrifuged at 1000 rpm. The cell pellet was dissolved again in sterile PBS and centrifuged at 1000 rpm as a period of washing. The pellet was hypotonically lysed in 10mM HEPES buffer by passing through a sterile syringe 10 times. This lysate was used for standard IDO1 assay as mentioned earlier [31]. The results showed that 20 ng/mL of human IFN-γ is sufficient enough to show that activity in the cellular conditions. Therefore all cell works were performed using this concentration of IFN-γ. After that, the cells were treated with human IFN-γ (20 ng/mL) in complete media for a period of 48 h. This treatment is reported to allow over-expression of IDO1 enzyme in MDA-MB-231 cells [31]. Next, the cells were treated with appropriate concentrations of the compounds (20 nM, 50 nM, 100 nM and 500 nM) for a period of 4 h. Following this, 150 μM tryptophan was added and treated for additional period of 5 h. Cells stimulated with IFN-γ alone served as negative control while cells stimulated with IFN-γ and then with 150μM tryptophan served as positive control. Post treatment phase, the cells were washed with sterile cell-culture grade PBS and were trypsinized and centrifuged at 1000 rpm. The cell pellet was dissolved again in sterile PBS and centrifuged at 1000 rpm as a period of washing. The pellet was hypotonically lysed in 10mM HEPES buffer by passing through a sterile syringe 10 times. This lysate was used for standard IDO1 assay as mentioned earlier [3, 26, 28]. IC_{50} values were determined for each inhibitor accordingly.

4.12. *MTT assay and morphological analysis*

The dye MTT (3-(4,5-Dimethylthiazol-2-yl)-2,5-Diphenyltetrazolium Bromide) was used to measure cellular viability. 10,000 cells were seeded overnight in 96 well plate in total volume of 0.2 mL DMEM/F12 complete medium [35]. After 12 hours cells were washed twice with cell culture grade phosphate buffer saline (PBS) and were incubated with the IDO1 inhibitors (at IC_{50} and 2 × IC_{50} values respectively) in 0.2 mL of DMEM/F12serum free medium (incomplete medium) for 24 h and 48 h. Cells treated with incomplete medium alone were considered as 100% viable. After the treatment period, the cells were washed twice with PBS and taken for morphological analysis via cytell imaging system (GE Healthcare). Images were collected at 10X magnification. After imaging, each well was incubated with 100µL of MTT (0.5 mg/ml in PBS) for 4h at 37 °C with 5% CO_2. Then, MTT solution was removed and the formazan crystals were dissolved in 100µL cell culture grade DMSO. The absorbance was determined using a spectrophotometer (SpectraMax M2) at 570nm and 660nm (to subtract scattering effects of crystals).

4.13. *Expression and purification of human TDO enzyme*

The plasmid of human TDO (in the vector pET28a) was used for this study. The pET28a-TDO construct was a generous gift from Professor Emma Raven (University of Leicester). The pET28a-TDO plasmid was transformed in Rosetta (DE3) pLysS cells and used for over-expression of TDO enzyme [29]. The transformed cells were first grown at 30 °C and 120 rpm to an OD_{600} of 0.6 in LB medium containing 50 µg/mL of kanamycin. The culture was cooled down in an ice/water bath and the protein expression was induced

by the addition of IPTG (0.5 mM), 5-aminolevulinic acid (0.5 mM), hemin from bovine (7 μM). The culture was then grown 22 °C and 120 rpm for 20 h. Cells (1 L LB culture) were cooled down and collected by centrifugation at 5000 rpm for 10 min at 4 °C. The pellet was re-dissolved with PBS buffer at pH 7.4 containing 1 mM PMSF and collected by centrifugation at 15000 rpm for 10 min at 4 °C. The pellet was stored at -80 °C. After thawing, the cells were collected by centrifugation at 15000 rpm for 10 min at 4 °C. Cells were again suspended in 20 mL of 50 mM phosphate buffer at pH 8.0 containing 300 mM KCl, 10 mM imidazole and 10 mM $MgCl_2$ and 1 mM PMSF, protease inhibitors (complete EDTA free) and DNase (< 1 mg). The suspension was sonicated on ice for 10 min (30 s sonication followed by 30 s cooling) at maximum power. The cell debris was removed by centrifugation (at 20000 rpm for 30 min) and filtration on 0.22 μm filter. To the supernatant, 1 mL of nickel-nitrilotriacetic acid resin was added and the mixture was incubated on ice with gentle stirring (80 rpm) for 1 h. After that the mixture was poured onto a column filled with 20 mL of 50 mM phosphate buffer at pH 8.0 containing 300 mM KCl, 10 mM imidazole. After sequentially washing the nonspecifically bound protein with 50 ml of 50 mM phosphate buffer at pH 8.0, 300 mM KCl containing 20, 30 and 50 mM imidazole, respectively, the protein was eluted in five fractions using 50 mM phosphate buffer at pH 8.0 containing 300 mM KCl, 250 mM imidazole. 2 mL of the collected protein was then buffer exchanged into 50 mM Tris, pH 8.0, using a Sephadex-G25 column. Coomassie-blue stained SDS-PAGE gel image of the purified enzyme showed > 90% purity. The absorbance of the purified enzyme was also tested and the ratio of λ_{404} and λ_{280} was around 1.2.

4.14. *TDO inhibition assay*

The enzyme inhibition assay was performed according to the reported procedure [25, 27, 29]. The enzymatic reaction (500 μL) was performed in 100 mM potassium phosphate buffer at pH 8.0 using sodium-ascorbate (20 mM), catalase (240 nM), methylene blue (10 μM), purified recombinant TDO (20 nM), *L*-Trp (100 μM), DMSO (0.05%, v/v) and triton-X 100 (0.01 %, v/v). First, the assay was performed using the inhibitors at different concentrations of 100 nM to 10 μM and then repeated five times at a particular concentration. The reaction was performed at 37 °C for 1 h and quenched by addition of 30% (w/v) trichloroacetic acid (90 μL). The reaction mixture was incubated at 50 °C for 30 minutes and then centrifuged at 10000 rpm for 10 minutes to the supernatant 100 μL of 2% pDMAB in acetic acid was added and stored for 10 minutes. The amount of kynurenine was indirectly monitored by measuring absorbance at 480 nm, which correspond to the product of kynurenine and pDMAB. The IC_{50} values were calculated using this standard curve generated from pure kynurenine.

ASSOCIATED CONTENT

Supplementary Data

Supplementary data related to this article can be found at

Figures of mass spectral signal of compounds in different solutions, HPLC based activity assay data, Cytotoxicity data, mode of enzyme inhibition data, ^{1}H NMR and ^{13}C NMR spectra of the synthesized compounds.

Author Contribution

‡S.P. and A.R. contributed equally to this work.

Notes

The authors declare no competing financial interest.

Conflict of Interest

The authors declare that there are no conflicts of interest.

ACKNOWLEDGEMENTS

We gratefully acknowledge DST, Govt. of India (SB/FT/CS-131/2012) for financial support. We are thankful to Central Instrument Facility and Department of Chemistry and Ministry of Human Resource Development for Centre of Excellence in FAST (5-7/2014-TS-VII) for instrumental support.

REFERENCES

[1] U.F. Rohrig, S.R. Majjigapu, P. Vogel, V. Zoete, O. Michielin, Challenges in the Discovery of Indoleamine 2,3-Dioxygenase 1 (IDO1) Inhibitors, J. Med. Chem. 58 (2015) 9421-9437.

[2] M.H. Kershaw, J.A. Westwood, C.Y. Slaney, P.K. Darcy, Clinical application of genetically modified T cells in cancer therapy, Clin. Transl. Immunol. 3 (2014) e16.

[3] O. Takikawa, R. Yoshida, R. Kido, O. Hayaishi, Tryptophan Degradation in Mice Initiated by Indoleamine 2,3-Dioxygenase, J. Biol. Chem. 261 (1986) 3648-3653.

[4] S. Yamamoto, O. Hayaishi, Tryptophan pyrrolase of rabbit intestine. D- and L-tryptophan-cleaving enzyme or enzymes, J. Biol. Chem. 242 (1967) 5260-5266.

[5] B. Clement, Reduction of N-hydroxylated compounds: amidoximes (N-hydroxyamidines) as pro-drugs of amidines, Drug Metab. Rev. 34 (2002) 565-579.

[6] C. Uyttenhove, L. Pilotte, I. Theate, V. Stroobant, D. Colau, N. Parmentier, T. Boon, B.J. Van den Eynde, Evidence for a tumoral immune resistance mechanism

based on tryptophan degradation by indoleamine 2,3-dioxygenase, Nat. Med. 9 (2003) 1269-1274.

[7] J. Croitoru-Lamoury, F.M. Lamoury, M. Caristo, K. Suzuki, D. Walker, O. Takikawa, R. Taylor, B.J. Brew, Interferon-gamma regulates the proliferation and differentiation of mesenchymal stem cells via activation of indoleamine 2,3 dioxygenase (IDO), PLoS One 6 (2011) e14698.

[8] M. Platten, W. Wick, B.J. Van den Eynde, Tryptophan catabolism in cancer: beyond IDO and tryptophan depletion, Cancer Res. 72 (2012) 5435-5440.

[9] N. van Baren, B.J. Van den Eynde, Tryptophan-degrading enzymes in tumoral immune resistance, Front. Immunol. 6 (2015) 34.

[10] R. Riesenberg, C. Weiler, O. Spring, M. Eder, A. Buchner, T. Popp, M. Castro, R. Kammerer, O. Takikawa, R.A. Hatz, C.G. Stief, A. Hofstetter, W. Zimmermann, Expression of indoleamine 2,3-dioxygenase in tumor endothelial cells correlates with long-term survival of patients with renal cell carcinoma, Clin. Cancer Res.13 (2007) 6993-7002.

[11] M.P. Heyes, K. Saito, J.S. Crowley, L.E. Davis, M.A. Demitrack, M. Der, L.A. Dilling, J. Elia, M.J. Kruesi, A. Lackner, et al., Quinolinic acid and kynurenine pathway metabolism in inflammatory and non-inflammatory neurological disease, Brain 115 (Pt 5) (1992) 1249-1273.

[12] M.C. Wichers, M. Maes, The role of indoleamine 2,3-dioxygenase (IDO) in the pathophysiology of interferon-alpha-induced depression, J. Psychiatry Neurosci. 29 (2004) 11-17.

[13] S. Vazquez, N.R. Parker, M. Sheil, R.J. Truscott, Protein-bound kynurenine decreases with the progression of age-related nuclear cataract, Invest. Ophthalmol. Vis. Sci. 45 (2004) 879-883.

[14] A.M. Sardar, G.P. Reynolds, Frontal cortex indoleamine-2,3-dioxygenase activity is increased in HIV-1-associated dementia, Neurosci. Lett. 187 (1995) 9-12.

[15] A. Okamoto, T. Nikaido, K. Ochiai, S. Takakura, M. Saito, Y. Aoki, N. Ishii, N. Yanaihara, K. Yamada, O. Takikawa, R. Kawaguchi, S. Isonishi, T. Tanaka, M. Urashima, Indoleamine 2,3-dioxygenase serves as a marker of poor prognosis in gene expression profiles of serous ovarian cancer cells, Clin. Cancer Res. 11 (2005) 6030-6039.

[16] W.P. Malachowskia, M. Wintersa, J.B. DuHadawayb, A. Ariel Lewis-Ballestere, S. Badira, J. Waia, M. Rahmana, E. Sheikha, J.M. LaLondea, S.R. Yehe, G.C. Prendergastb, A.J. Muller, O-alkylhydroxylamines as rationally-designed mechanism-based inhibitors of indoleamine 2,3-dioxygenase-1, Eur. J. Med. Chem. 108 (2016) 564–576.

[17] R. Pasceri, D. Siegel, D. Ross, C.J. Moody, Aminophenoxazinones as Inhibitors of Indoleamine 2,3-Dioxygenase (IDO). Synthesis of Exfoliazone and Chandrananimycin A, J. Med. Chem. 56 (2013) 3310-3317.

[18] E. Vacchelli, F. Aranda, A. Eggermont, C. Sautes-Fridman, E. Tartour, E.P. Kennedy, M. Platten, L. Zitvogel, G. Kroemer, L. Galluzzi, Trial watch: IDO inhibitors in cancer therapy, Oncoimmunology 3 (2014).

[19] F. Qian, J. Villella, P.K. Wallace, P. Mhawech-Fauceglia, J.D. Tario, C. Andrews, J. Matsuzaki, D. Valmori, M. Ayyoub, P.J. Frederick, A. Beck, J.Q. Liao, R. Cheney, K. Moysich, S. Lele, P. Shrikant, L.J. Old, K. Odunsi, Efficacy of Levo-

1-Methyl Tryptophan and Dextro-1-Methyl Tryptophan in Reversing Indoleamine-2,3-Dioxygenase-Mediated Arrest of T-Cell Proliferation in Human Epithelial Ovarian Cancer, Cancer Res. 69 (2009) 5498-5504.

[20] E.W. Yue, B. Douty, B. Wayland, M. Bower, X.D. Liu, L. Leffet, Q. Wang, K.J. Bowman, M.J. Hansbury, C.N. Liu, M. Wei, Y.L. Li, R. Wynn, T.C. Burn, H.K. Koblish, J.S. Fridman, B. Metcalf, P.A. Scherle, A.P. Combs, Discovery of Potent Competitive Inhibitors of Indoleamine 2,3-Dioxygenase with in Vivo Pharmacodynamic Activity and Efficacy in a Mouse Melanoma Model, J. Med. Chem.52 (2009) 7364-7367.

[21] A.M. Malinen, M. NandyMazumdar, M. Turtola, H. Malmi, T. Grocholski, I. Artsimovitch, G.A. Belogurov, CBR antimicrobials alter coupling between the bridge helix and the beta subunit in RNA polymerase, Nat. Comm. 5 (2014).

[22] Y.J. Wang, J. Rong, B. Zhang, L.M. Hu, X.L. Wang, C.C. Zeng, Design and synthesis of N-methylpyrimidone derivatives as HIV-1 integrase inhibitors, Bioorg. Med. Chem. 23 (2015) 735-741.

[23] J. Cai, H.T. Wei, K.H. Hong, X.Q. Wu, M. Cao, X. Zong, L.S. Li, C.L. Sun, J.Q. Chen, M. Ji, Discovery and preliminary evaluation of 2-aminobenzamide and hydroxamate derivatives containing 1,2,4-oxadiazole moiety as potent histone deacetylase inhibitors, Eur. J. Med. Chem. 96 (2015) 1-13.

[24] Y.D. Zhuang, P.Y. Chiang, C.W. Wang, K.T. Tan, Environment-Sensitive Fluorescent Turn-On Probes Targeting Hydrophobic Ligand-Binding Domains for Selective Protein Detection, Angew. Chem. Int. Ed. 52 (2013) 8124-8128.

[25] O. Takikawa, T. Kuroiwa, F. Yamazaki, R. Kido, Mechanism of Interferon-Gamma Action - Characterization of Indoleamine 2,3-Dioxygenase in Cultured Human-Cells Induced by Interferon-Gamma and Evaluation of the Enzyme-Mediated Tryptophan Degradation in Its Anticellular Activity, J. Biol. Chem. 263 (1988) 2041-2048.

[26] U.F. Rohrig, L. Awad, A. Grosdidier, P. Larrieu, V. Stroobant, D. Colau, V. Cerundolo, A.J.G. Simpson, P. Vogel, B.J. Van den Eynde, V. Zoete, O. Michielin, Rational Design of Indoleamine 2,3-Dioxygenase Inhibitors, J. Med. Chem. 53 (2010) 1172-1189.

[27] C.J.D. Austin, J. Mizdrak, A. Matin, N. Sirijovski, P. Kosim-Satyaputra, R.D. Willows, T.H. Roberts, R.J.W. Truscott, G. Polekhina, M.W. Parker, J.F. Jamie, Optimised expression and purification of recombinant human indoleamine 2,3-dioxygenase, Protein Express. Purif.37 (2004) 392-398.

[28] U.F. Rohrig, S.R. Majjigapu, A. Grosdidier, S. Bron, V. Stroobant, L. Pilotte, D. Colau, P. Vogel, B.J. Van den Eynde, V. Zoete, O. Michielin, Rational Design of 4-Aryl-1,2,3-Triazoles for Indoleamine 2,3-Dioxygenase 1 Inhibition, J. Med. Chem. 55 (2012) 5270-5290.

[29] J.S. Wu, S.Y. Lin, F.Y. Liao, W.C. Hsiao, L.C. Lee, Y.H. Peng, C.L. Hsieh, M.H. Wu, J.S. Song, A. Yueh, C.H. Chen, S.H. Yeh, C.Y. Liu, S.Y. Lin, T.K. Yeh, J.T.A. Hsu, C. Shih, S.H. Ueng, M.S. Hung, S.Y. Wu, Identification of Substituted Naphthotriazolediones as Novel Tryptophan 2,3-Dioxygenase (TDO) Inhibitors through Structure-Based Virtual Screening, J. Med. Chem. 58 (2015) 7807-7819.

[30] L.F. Yu, Y.Y. Li, M.B. Su, M. Zhang, W. Zhang, L.N. Zhang, T. Pang, R.T. Zhang, B. Liu, J.Y. Li, J. Li, F.J. Nan, Development of Novel Alkene Oxindole Derivatives As Orally Efficacious AMP-Activated Protein Kinase Activators, Acs Med. Chem. Lett. 4 (2013) 475-480.

[31] M.T. Travers, I.F. Gow, M.C. Barber, J. Thomson, D.B. Shennan, Indoleamine 2,3-dioxygenase activity and L-tryptophan transport in human breast cancer cells, Biochim. Biophys. Acta 1661 (2004) 106-112.

[32] S.S. Yang, X.S. Li, F.F. Hu, Y.L. Li, Y.Y. Yang, J.K. Yan, C.X. Kuang, Q. Yang, Discovery of Tryptanthrin Derivatives as Potent Inhibitors of Indoleamine 2,3-Dioxygenase with Therapeutic Activity in Lewis Lung Cancer (LLC) Tumor-Bearing Mice, J. Med. Chem. 56 (2013) 8321-8331.

[33] S. Tojo, T. Kohno, T. Tanaka, S. Kamioka, Y. Ota, T. Ishii, K. Kamimoto, S. Asano, Y. Isobe, Crystal Structures and Structure Activity Relationships of Imidazothiazole Derivatives as IDO1 Inhibitors, Acs Med. Chem. Lett. 5 (2014) 1119-1123.

[34] N. Mamidi, R. Borah, N. Sinha, C. Jana, D. Manna, Effects of ortho substituent groups of protocatechualdehyde derivatives on binding to the C1 domain of novel protein kinase C, J. Phys. Chem. B 116 (2012) 10684-10692.

[35] P. Kumar, S. Gorai, M.K. Santra, B. Mondal, D. Manna, DNA binding, nuclease activity and cytotoxicity studies of Cu(II) complexes of tridentate ligands, Dalton Transac. 41 (2012) 7573-7581.

Highlights

- Synthesis of benzofurazan derivatives of *N′*-hydroxyoximidines as IDO1 inhibitors.
- Inhibition activities were demonstrated by spectroscopic and HPLC-based methods.
- Stronger inhibition with halogen substituted *N′*-hydroxyoximidine derivatives.
- Higher selectivity for IDO1 enzyme over TDO enzyme.
- Nanomolar-level IDO1 inhibition potency with low toxicity in cells.